Integration of genetic fine-mapping and multi-omics data reveals candidate effector genes for hypertension

Stefan van Duijvenboden[1,2,3*], Julia Ramírez[1,4,5*], William J. Young[1,6], Kaya J. Olczak[1], Farah Ahmed[1], Mohammed J.A.Y. Alhammadi[7,], International Consortium of Blood Pressure[†], Christopher G. Bell[1‡], Andrew P. Morris[8,9‡], & Patricia B. Munroe[1,10‡]

[1]William Harvey Research Institute, Barts and the London Faculty of Medicine and Dentistry, Queen Mary University of London, London, EC1M 6BQ, U.K.

[2]Institute of Cardiovascular Science, University College London, London, U.K.

[3]Nuffield Department of Population Health, University of Oxford, Oxford, U.K.

[4]Aragon Institute of Engineering Research, University of Zaragoza, Spain.

[5]Centro de Investigación Biomédica en Red – Bioingeniería, Biomateriales y Nanomedicina, Spain.

[6]Barts Heart Centre, St Bartholomew's Hospital, London, EC1A 7BE, U.K.

[7]Khalifa University, Abu Dhabi, United Arab Emirates.

[8]Centre for Genetics and Genomics Versus Arthritis, Centre for Musculoskeletal Research, The University of Manchester, Manchester, U.K.

[9]National Institute of Health and Care Research, Manchester Biomedical Research Centre, Manchester University NHS Foundation Trust, Manchester Academic Health Science Centre, Manchester, U.K.

[10]National Institute of Health and Care Research, Barts Cardiovascular Biomedical Research Centre, Queen Mary University of London, London, EC1M 6BQ, U.K.

*These first authors contributed equally

[†]Membership of the consortium is listed in the Supplementary Material

[‡]These authors directed the study equally

Abstract

Genome-wide association studies of blood pressure (BP) have identified >1000 loci but the effector genes and biological pathways at these loci are mostly unknown. Using published meta-analysis summary statistics, we conducted annotation-informed fine-mapping incorporating tissue-specific chromatin segmentation to identify causal variants and candidate effector genes for systolic BP, diastolic BP, and pulse pressure. We observed 532 distinct signals associated with ≥2 BP traits and 84 with all three. For >20% of signals, a single variant accounted for >75% posterior probability, 65 were missense variants in known (*SLC39A8*, *ADRB2, DBH*) and previously unreported BP candidate genes (*NRIP1*, *MMP14*). In disease-relevant tissues, we colocalized >80 and >400 distinct signals for each BP trait with *cis*-eQTLs, and regulatory regions from promoter capture Hi-C, respectively. Integrating mouse, human disorder, tissue expression data and literature review, we provide consolidated evidence for 394 BP candidate genes for future functional validation and identifies several new drug targets.

Introduction

Elevated blood pressure (BP) affects over 1 billion people and is one of the most important risk-factors for cardiovascular disease (CVD), leading to significant mortality and morbidity worldwide[1]. It is estimated to cause more than 10 million deaths per year[2]. Genome-wide association studies (GWAS), bespoke targeted arrays (Cardio Metabochip) and Exome-array wide association studies (EAWAS) have identified over 1,000 BP-associated loci for this heritable polygenic trait[3-8]. However, for most loci, the effector genes and relevant biological processes through which BP associations are mediated have yet to be characterised. Here, we use published GWAS meta-analysis results (n >757,000) of systolic BP (SBP), diastolic BP (DBP) and pulse pressure (PP)[3] to perform fine mapping of causal variants at BP loci. Through the integration of GWAS with tissue specific epigenomic annotations, and colocalisation of BP associations with expression quantitative loci (eQTLs) and Hi-C promoter interactions in relevant BP tissues, we identify high confidence effector genes and causal pathways, and assess their potential for drag target identification or repurposing opportunities

Results

Study overview and reporting of loci

We utilised previously reported meta-analyses of GWAS of BP traits in up to 757,601 individuals of European ancestry from the International Consortium of BP and UK Biobank (ICBP+UKBB)[3]. Each contributing GWAS had been imputed up to reference panels from the 1000 Genomes Project[9,10] and/or Haplotype Reference Consortium[11]. After quality control, meta-analysis association summary statistics for SBP, DBP and PP were reported for up to 7,160,657 single nucleotide variants (SNVs). An overview of the study design is provided in Supplementary Figure 1.

We considered a total of 606 genomic regions encompassing previously reported lead SNVs for SBP, DBP or PP that attained genome-wide significance ($P < 5x10^{-8}$) for at least one BP trait (**Methods**, Supplementary Table 1). Through approximate cross-trait conditional analyses (**Methods**), we partitioned BP associations at the 606

genomic regions into a total of 1,850 distinct signals that were associated with at least one BP trait at genome-wide significance (Figure 1, Supplementary Table 2). Of these signals, 532 were associated with at least two BP traits (333 with SBP and DBP, 267 with SBP and PP, and 100 with DBP and PP), and 84 were associated with all three traits. The only discordancy in direction of effect was for 17 of the 100 signals shared across DBP and PP , where the DBP increasing allele was the PP decreasing allele).

The cross-trait approximate conditional analyses revealed several genomic regions with complex patterns of associations with SBP, DBP and PP. For six genomic regions, more than 20 distinct signals of association were observed for at least one BP trait. The most complex associations were observed across: (i) a 6.4Mb region of chromosome 17, encompassing previously reported loci that include *PLCD3*, *GOSR2*, *HOXB7*, *ZNF652*, and *PHB* (locus ID 576, 37 distinct signals); (ii) a 5.8Mb region of chromosome 10, encompassing previously reported loci that include *PAX2*, *CYP17A1*, *NT5C2*, and *OBFC1* (locus ID 403, 34 distinct signals); and (iii) the major histocompatibility complex region of chromosome 6 (5.7Mb, locus ID 251, 32 distinct signals) that encompasses previously reported loci that include *BAT2*, *BAT5*, and *HLA DQB1*.

Fine-mapping and genomic annotation reveals high-confidence causal variants for BP traits

Previous studies have demonstrated that improved localisation of causal variants driving association signals for complex human traits can be attained by integrating GWAS data with genomic annotation[12]. By mapping SNVs to functional and regulatory annotations from GENCODE[13,14] and the Roadmap Epigenomics Consortium[15] (**Methods**), we observed significant joint enrichment ($P < 0.0002$, Bonferroni correction for 253 annotations) for BP associations mapping to protein coding exons and 3' UTRs, enhancers in heart and adrenal gland, and promoters in adipose and heart (Supplementary Table 3, Supplementary Figure 2).

For each distinct signal, we then derived credible sets of variants that together account for 99% of the posterior probability (π) of driving the BP trait association under an annotation-informed prior model of causality in which SNVs mapping to the genomic annotations in the globally enriched signatures for SBP, DBP and PP are upweighted

(**Methods**). The median 99% credible set size was 20 variants for SBP and DBP, and 22 for PP (Supplementary Table 4). For 208 (24%), 224 (24.8%) and 159 (22.9%) SBP, DBP and PP signals, respectively, a single SNV accounted for more than 75% of the posterior probability of driving the BP association under the annotation-informed prior, which we defined as "high-confidence" for causality (Figure 2, Supplementary Table 5).

High-confidence SNVs are enriched for BP-related phenotypes

We used the Genomic Regions Enrichment of Annotations Tool (GREAT) v4.0.4[16] (**Methods**) to explore the potential biological impact of all high confidence SNVs through their enrichment within trait-related genomic regions including *cis*-regulatory elements (CREs). We explored SNVs separately for the three BP traits and physiologically consistent enrichment results were identified for these location data for Gene Ontology Biological Processes (e.g., circulatory system processes, regulation of BP), Human Phenotype (e.g., abnormality systemic blood pressure, abnormality of vasculature), Mouse Phenotype and Knockout data (e.g., abnormal blood vessel morphology, increased systemic arterial blood pressure) (Supplementary Figure 3 and Supplementary Table 6).

Missense variants implicate causal candidate genes

We identified 65 high-confidence missense variants for BP association signals (Supplementary Table 7). Among these, 20 were driving the same association signal across two BP traits, and one (*RGL3* p.Pro162His) was driving the same association signal across all three BP traits (Table 1). *RGL3* is not well characterised, but several missense variants in the gene have been previously identified in BP EAWAS[7]. In our study, three distinct association signals are driven by *HFE* missense variants (*HFE* p.His63Asp, *HFE* p. Ser65Cys and *HFE* p.Cys282Tyr). These variants are associated with predisposition to hereditary hemochromatosis, of which, portal hypertension and restrictive diastolic function are recognised phenotypes [17].

Fifteen missense variants were, in fact, identified to have a posterior probability of >99.9% of driving distinct BP association signals. These variants implicate several well characterised BP genes (including *SLC39A8* p.Ala391Thr; *ADRB2* p.Gly16Arg and p.Thr164Ile; and *DBH* p.Arg549Cys), but also highlight less well-established candidate

genes, including *NRIP1*, *MMP14* and *PLCB3*. *NRIP1* is a regulator of the mineralocorticoid receptor, and *MMP14* is an endopeptidase with a key role in degrading components of the extracellular matrix and regulation of blood vessel stability[18]. EAWAS have identified missense variants in *PLCB3* to be associated with BP traits[7], a gene that encodes an enzyme involved in intracellular signal transduction found to be increased in a mouse model of hypertension and hypertrophy[19].

Several high-confidence missense variants implicate genes associated with kidney traits/disorders including *NCOA7* p. Ser399Ala, *LAMB2* p. Ala1765Thr and *NPHS2* p. Arg229Gln. *NCOA7* encodes the nuclear receptor coactivator 7, a vacuolar proton pumping ATPase (V-ATPase) interacting protein. It is highly expressed in the kidney with knock out mice observed to have lower BP[20]. *LAMB2* encodes beta chain isoform laminin, and mutations in this gene cause Pierson syndrome (OMIM# 609049), a congenital nephrotic syndrome, in which the phenotype includes hypertension[21]. Mutations in *NPHS2* cause steroid-resistant nephrotic syndrome[22].

Non-coding BP association signals map to trait-related transcription factor binding sites

Whilst the high-confidence missense variants identified have directly interpretable effects, the majority of the posterior probability of causality for BP trait associations maps to non-coding sequence. To explore these high-confidence non-coding SNVs, we firstly sought evidencefor enrichment of transcription factor binding site (TFBS) motifs. We interrogated sets of sequences obtained by expanding 10bp either side of these SNVs for each of the three traits (see **Methods**). This identified significant enrichment for 7 SBP, 10 DBP, and 5 PP TFBS motifs that were partially overlapping (Supplementary Table 8). The motif for *PAX2* was significant across all three traits (top corrected $P = 2.8 \times 10^{-25}$ for DBP), with this transcription factor involved in nephron development, as well as implicated in monogenic renal abnormalities[23].

Effector genes identified using gene expression in disease relevant tissues

To gain further insight into mechanisms through which non-coding association signals are mediated, where identification of the cognate effector gene is challenging[12], we integrated genetic fine-mapping data with expression quantitative trait loci (*cis*-eQTL) in disease relevant tissues from the GTEx Consortium[24]. The tissues included were

adipose, adrenal gland, artery, kidney cortex, heart, nerve, and brain. We observed convincing support for colocalization with eQTLs (**Methods)** for 96 SBP, 107 DBP and 84 PP signals (Supplementary Table 9). In total, 54 (56%), 58 (54%), and 41 (49%) of the signals colocalized with an eQTL for a single gene in at least one tissue. Across all traits, there was a total of 135 genes with tissue-specific colocalizations, of which 55 (41%) were in arterial tissues, 35 (26%) were in nerve or brain tissues, 21 (16%) were in adipose tissue, 13 (10%) were in heart, 9 (7%) were in adrenal, and 2 (1%) were in kidney.

Of the signals associated with all three BP traits, nine colocalized with an eQTL for a single effector gene. These were: *AGT* (brain cerebellum), *ARHGAP24* (tibial artery and aorta), *ARHGAP42* (tibial artery, aorta, and adipose), *CHD13* (aorta), *CTD-2336O2.1* (brain tissues), *FES* (tibial artery), *FGF5* (kidney cortex), *IGFBP3* (heart left ventricle), and *JPH2* (adrenal gland). Three genes (*AGT*, *ARHGAP42* and *IGFBP3*) have known or supporting data for a role in BP regulation. *AGT* encodes angiotensinogen, a substrate of the renin-angiotensinogen system – a key regulatory pathway[25]. *ARHGAP42* is selectively expressed in smooth muscle cells and modulates vascular resistance, and a knockout *Arhgap42* mouse model demonstrates salt mediated hypertension[26]. *IGFBP3*, which encodes the insulin growth factor binding protein 3, has data supporting association with BP and CVD phenotypes, and a knockout mouse model has increased ventricular wall thickness and shortened ST segment[27]. It also modulates insulin growth factor 1 (IGF-1)bioactivity with potential regulation of vascular tone *in-vivo* through NO release[28]. Additionally, there is a high-confidence missense variant implicating *IGFBP3,* highlighting distinct associations mediated by the same gene but through different underlying biological processes. Other colocalized effector genes demonstrate links to cardiovascular phenotypes (*FES*[29], *FGF5*[30], and *JPH2*[31]) but have not yet been functionally characterised.but demonstrate links to cardiovascular phenotypes.

We observed many individual loci with several distinct signals for each BP trait that colocalized with eQTLs for different genes. The genomic region on chromosome 12 encompassing *HDAC7*, *H1FNT*, *CCDC65*, *PRKAG1*, *AM186B*, *CERS5*, and *DIP2B*, spans 3.5Mb, and includes 11 signals for SBP, 12 for DBP and 5 for PP. Three signals colocalized with eQTLs and indicate two effector genes. One signal (associated with

both SBP and DBP) colocalized with an eQTL for *CACNB3* (adipose, tibial nerve and artery), which encodes a regulatory beta subunit of the voltage-dependent calcium channel. The regulatory subunit of the voltage-gated calcium channel gives rise to L-type calcium currents[32]. A *CACNB3* knock-out mouse model has a cardiovascular phenotype that includes abnormal vascular smooth muscle cell hypertrophy, increased heart weight and increased SBP and DBP[33]. A second signal, associated with DBP colocalized with an eQTL for *RP4-605O3.4* (heart left ventricle), and a third signal (associated with SBP) colocalized with an eQTL in brain and heart left ventricle for this predicted gene.

A genomic region on chromosome 17 spanning 6.4Mb, which encompasses associations reported in several previous BP GWAS[3,7,34,35],includes 19 SBP, 16 DBP and 15 PP signals (Supplementary Table 2). Colocalization of signals with eQTLs implicates six effector genes (*DCAKD*, *NMT1*, *RP11-6N17.4*, *PNPO*, *PRR15LA* and *ZNF652*). Three independent signals colocalized with eQTLs for *NMT1* in brain. The *NMT1* gene encodes N-myristoyltransferase, which catalyses the transfer of myristate from CoA to proteins, and there is no clear association with cardiovascular disease. However, the Malacards database indicates an association with Patent Foramen Ovale, a common post-natal defect of cardiac atrial septation[36]. One DBP signal colocalized with an eQTL for *DCAKD* in adipose and nerve tissues. PP signals colocalized with eQTLs for *RP11-6N17.4* and *PNPO* in brain tissues. *PNPO* encodes pyridoxamine 5'-phosphate oxidase, an enzyme in the rate limiting step in vitamin B6 synthesis. Deficiency of PNPO primarily results in seizures, with many systemic symptoms including cardiac abnormalities[37]. We also observed a SBP signal that colocalized with an eQTL for *PRR15LA* in tibial artery, and a signal associated with both with SBP and DBP that colocalized with an eQTL for *ZNF652* in adipose tissue.

At a second genomic region on chromosome 17 encompassing *MRC2*, *ACE*, *PECAM1*, and *MILR1*, we observed four signals for SBP, three for DBP and four for PP (Supplementary Table 2), of which three signals colocalized with different genes across multiple tissues (Figure 3). One SBP signal colocalizes with an eQTL for *MRC2* in tibial artery. *MRC2* encodes the mannose receptor C type 2 and plays a role in extracellular matrix remodelling[38]. A signal associated with both SBP and DBP colocalized with an eQTL for *ACE* in kidney, adipose, and brain tissues. *ACE* encodes

the angiotensin-converting enzyme, a central component of the renin–angiotensin–aldosterone system[39]. A third SBP signal colocalized with an eQTL for two genes across several tissues: *DDX5* (arteries, brain and tibial nerves) and *CEP95* (tibial nerve and arteries). These genes have little prior association with cardiovascular phenotypes. *DDX5* encodes DEAD-Box Helicase 5, which is thought to be a coregulator of transcription or splicing, and recent data indicates a role in smooth muscle cell protection and neointimal hyperplasia[40]. Homozygous *Ddx5* knockout mice die at embryonic day 11.5 and demonstrate blood vessel abnormalities. There is little information on *CEP95*, which encodes centrosomal protein 95, although differential gene expression was observed in spontaneously hypertensive rats[41].

Identification of effector genes using promotor-centered long-range chromatin interactions in disease relevant tissues

To explore possible long-range enhancer influence on specific target genes, we integrated genetic fine-mapping data with potential functional CREs identified to target the promoters of well-annotated protein-coding genes via long-range chromatin interactions (capture Hi-C data from Jung et al.[42]). Promoter interactions and candidate genes were identified for 629 signals at 366 genomic regions (RegulomeDB Score ≤ 3) across adrenal gland, dorsolateral prefrontal cortex, hippocampus, aorta, left ventricle, right ventricle, and fat (Supplementary Table 10). We observed signals at 13 genomic regions that included 99% credible set variants with regulatory potential across SBP and DBP, for which several potential target genes of the regulatory variants were indicated. At five signals, one gene was indicated in a single tissue: *ACTRT2* (dorsolateral prefrontal cortex), *ARMC4* (right ventricle), *AP001024.1* (hippocampus), *TBX3* (aorta) and *YES1* (hippocampus). At other genomic regions , many genes in one tissue were indicated: *HOXA5*, *HOXA6* and *HOXA3* (adrenal gland), *RP11691N7.6*, *C11orf31*, *TIMM10*, *CLP1*, *YPEL4*, *ZDHHC5*, *FAM111A*, *TIMM10*, *AP001350.1*, *GLYATL2*, *GLYATL1* (hippocampus, dorsolateral prefrontal cortex), and *ABHD17C*, *MESDC2* (two brain tissues). At three signals, more than one gene in more than one tissue were highlighted, such as *GPR124*, *DDHD2*, *FGFR1*, *PPAPDC1B*, *LETM2*, *TACC1* (two brain tissues, adrenal gland, aorta, and right ventricle). Candidate genes at three signals have existing functional data supporting an association with BP or cardiovascular traits: *HOXA3*, *ADM* and *TBX3*[27,43,44].

We next explored whether signals that colocalized with eQTLs for effector genes overlapped with those implicated by Hi-C predicted promoter interactions. We focused on the 80 signals that have support for colocalization with eQTLs in relevant tissues across all traits (Supplementary Table 11). For 34 signals, the effector gene indicated by Hi-C was the same as that identified via colocalization with the eQTLs, and for 15 of these signals the same gene and tissue was implicated (Supplementary Table 12). The 15 candidate genes were: *AKR1B1*, *ASAP2, COL27A1, IRF5, MAP1B, MRPS6, MXD3, RAD52, RERE, RNF130, SLC5A3*, *SLC20A2, TNS3, TRIOBP*, and *USP36*. A review of the 15 genes indicates knock-out mouse models of three effector genes (*COL27A1, RERE*, and *SLC20A2*) have cardiovascular abnormalities – these genes have not previously been highlighted as potential candidate genes for hypertension (Supplementary Table 12).

To explore our Hi-C predicted promoter interactions more broadly, we additionally probed our results to see whether there was also support for these potential CREs to target the same effector gene through a completely different prediction methodology from the recent EpiMap analysis[45]. This method is based on an active chromatin correlation with target gene expression. Several physiologically relevant candidate effector transcripts were highlighted, where the two methods predicted the same target for the same SNV in the same tissue or organ (See Supplementary Table 13). Potential targets included genes previously identified as highly plausible trait-related candidates from previous analyses, including *CLIC4*, *TNS1*, and *FERMT2*[46]. Target genes with presently unknown potential roles in SBP and DBP pathophysiology were also identified. These included two active CREs found in brain-related tissue, which would be of interest to explore for additional activity in potentially more physiologically relevant non-assayed tissues: *SHMT1*, the serine hydroxymethyltransferase 1 enzyme involved in folic acid metabolism associated, although inconsistently, with hypertension-related stroke[47] and *PLXNB2*, the Plexin-B2 transmembrane receptor that has an identified role in the developing kidney[48]. For PP this comprised, amongst others, some interesting target genes including *MYH11*, the smooth muscle myosin heavy chain 11 gene, with CRE activity in aortic tissue. Mutations within this gene lead to an autosomal dominant aortic aneurysm and dissection disorder (*AAT4*, OMIM #132900) with altered aortic stiffness[49,50]. Also, *COL6A3*, which encodes the alpha-3

chain of type VI collagen, was a target identified in heart tissue. This collagen gene is important in the developing mammalian heart[51] and is a causative gene in monogenic myopathy and dystonia diseases (OMIM: #158810; #254090; #616411)[52].

Consolidated effector gene evidence

Using complementary fine mapping and computational approaches (high-confidence missense, colocalised eQTLs and Hi-C interactions) we identified 956 candidate genes for SBP, 900 candidate genes for DBP and 773 candidate genes for PP with at least one line of evidence indicating a putative effector gene (Supplementary Tables 14-16).

We next looked for additional supportive evidence for each gene by combining information from mouse model data, human cardiovascular and renal phenotypes, and differential gene and protein expression across cardiovascular tissues (Methods). We selected as consolidated effector genes those which had two or more additional lines of evidence. In total, 197 SBP, 184 DBP and 180 PP genes were identified (Supplementary Tables 17-19), which together reflect 394 unique candidate genes.To gain insights into the biological role of these consolidated evidence effector genes for each BP trait we performed gene-set enrichment analyses. We found significant enrichment for 390, 333, and 299 gene ontology (GO) biological processes for SBP, DBP, and PP respectively (following removal of redundant processes, see Methods). There were 629 unique GO ID terms across the three traits, with 153, 106 and 103 unique to SBP, DBP and PP respectively. In total, 141 pathways were associated with two BP traits and 126 pathways with all three BP traits (Supplementary Tables 20-22). Some of the pathways associated with all three BP traits included: blood vessel remodelling, regulation of the immune system, circulatory and renal system processes, sodium ion transport and ion homeostasis, aging, smooth muscle cell migration, lipid metabolism processes and cytoskeletal organisation – all processes previously highlighted as important in BP control. The most significant SBP unique processes included: neurogenesis (P =1.9 x 10^{-17}), heart development (P = 1.2 x 10^{-11}) and regulation of cell death (P = 3.4 x 10^{-7}); for DBP, embryonic organ development (P = 5.0 x 10^{-11}) and positive regulation of RNA biosynthetic processes (P = 1.1 x 10^{-9}); and, for PP, muscle organ development (P = 5.1 x 10^{-9}) and trabecular formation (P = 0.007) and morphogenesis (P = 0.004).

347

348 *Drug target identification and repositioning opportunities*

349 We assessed the druggability of the consolidated candidate effector genes for each
350 BP trait via the druggable genome dataset from Finan et al.[53] (Supplementary Table
351 23, see Methods). We observed DBP to have a greater number of candidate effector
352 genes that encode proteins that are the main drug targets for anti-hypertensive
353 medications (*ACE*, *ADRA1A*, *ADRB1* and *NR3C2*), compared with SBP (*ACE*) and
354 PP (none). For several effector genes that are targets of existing drugs, there was
355 support as potential therapeutic targets for hypertension (e.g., *AKR1B1, PDE3A* and
356 *MAP2K1*). *AKR1B1* (aldo-keto reductase family 1 member B) is a target of aldose
357 reductase inhibitors that have been investigated for use in diabetes and also have
358 effects on BP[54]. *PDE3A* (phosphodiesterase 3A) is a target for hypertension with
359 bracydactyly, a rare autosomal dominant disorder and there is recent data indicating
360 several common variant associations also in the general population[7,55]. *PDE3A* is
361 targeted by several existing drugs, including Cilostazol (peripheral vascular disease),
362 Levosimendan for intravenous therapy for acutely decompensated heart failure and
363 Enoximone (pulmonary hypertension). There are no data currently indicating the use
364 of *PDE3A* inhibitors for hypertension, however a recent study suggests activation of
365 *PDE3A* in the heart may protect it from hypertrophy and failure[56]. *MAP2K1* (*MEK1*) is
366 a target of anti-neoplastic agents (*MAP2K1* is altered in 1% of lung and head and neck
367 squamous cell carcinomas)[57,58].The *MAPK* pathway is well recognised in BP control
368 and p38-MAPK inhibition has been considered previously as a therapeutic target
369 (which *MAP2K* activates). Our study applied rigorous multiple evidence methodology
370 employing differing datasets from the Evangelou et a to derive a consolidated effector
371 gene list.[3] This impacted the identification of potential therapeutic targets as we were
372 not able to replicate in our analysis the five candidate genes (*CA7, CACNA1C*,
373 *CACNB4, PKD2L1* and *SLC12A2*) reported in their paper as the target of anti-
374 hypertensive drug classes. However, *PKD2L1* did show individual Hi-C evidence as
375 bring the effector gene at the locus.

376

377 To further ascertain drug repositing opportunities, we tested for enrichment of these
378 consolidated candidate effector genes in clinical indication categories. We observed
379 significant enrichment of gene sets for cardiovascular and renal conditions

(Supplementary Table 24), with the results supporting the findings from interrogation of the Finan et al. druggable genome database.

Discussion

Strongly replicated human genetic associations with BP traits have been identified over the last decade. In this study, we have used a robust contemporary fine mapping pipeline to advance from these initial broadly associated genomic regions to the identification of hundreds of plausible previously-unreported effector genes (Figure 4). These candidates are now excellent targets for future focused functional validation.

We were able to localise approximately a quarter of all associations across all three BP traits to a single causal variant with >75% posterior probability. Of these high-confidence SNVs, 65 were missense variants, including 20 for two BP traits, and one in *RGL3* for all three traits. For the high confidence non-coding and potentially *cis*-regulatory variants, we employed pathogenic tissue-specific expression and chromatin conformation to identify their target genes. Of these SNVs, ~100 per trait colocalized with *cis*-eQTLs. Plausible effector genes included the well-known Angiotensin (*AGT*) and angiotensin converting enzyme (*ACE*), also more recently described genes from GWAS with functional data including sodium/potassium- transporting ATPase subunit beta-1 (*ATP1B1*) and Rho GTPase activating protein 42 (*ARHGAP42*). Other possible but less well functionally evaluated genes identified through eQTL analysis included *CDH13*, *FES*, *FGF5*, and *JPH2*.

We identified many loci with multiple complex signals within the same genomic region affecting different genes in different tissue types. Also, of note that whilst we observed high-confidence missense variants in kidney genes, as well as an enrichment for non-coding variants to overlap a nephron developmental TFBS, we identified only a very small proportion of eQTL colocalization in this tissue (*FGF5* and *ACE* and the lncRNA *AC021218.2*). This may reflect reduced power due to the relatively smaller numbers in GTEx for kidney than other tissues[24]. Using over 400 human kidneys and the same ICBP+UKBB GWAS dataset, Eales and colleagues reported nearly 31% of BP associated variants contained kidney eSNPs[59]. These results strongly emphasise the

413 importance of access to larger tissue banks for robust identification of all possible
414 effector genes.
415
416 Focusing on the overlap between the eQTL and Hi-C results in disease relevant
417 tissues identified a subset of 15 target genes identified in the same tissue. Of these,
418 the genes *COL27A1*, *RERE*, and *SLC20A2* also had supportive mouse data.
419 Furthermore, there is evidence that target genes consistently predicted across multiple
420 methods are the most robust[60]. We also explored overlap with the recent EpiMap[61],
421 highlighting, amongst others, *MYH11* and *COL6A3* as strong effector candidates for
422 PP. In total, our pipeline identified consolidated evidence effector genes for ~20% of
423 BP association signals (196 genes for 865 SBP associations; 184 genes for 904 DBP
424 associations; and 184 genes for 697 PP associations), an overview of the main
425 findings from the study are illustrated in Figure 4. Of the plausible BP genes, 14%
426 were identified to be drug targets, and several of these have good support for potential
427 repurposing for BP control.
428
429 The main strength of this work is that it combines robust GWAS associations, derived
430 from a powerfully large dataset, with comprehensive genetic annotation and tissue-
431 specific epigenomic maps derived from the Epigenomics Roadmap consortium. In the
432 exploration of the putative functional non-coding variants, a further strength was that
433 we were able to benefit from the expanded GTEx dataset[24], publicly available promoter
434 capture Hi-C data in pathogenically relevant tissues[42], as well as exploration of target
435 gene prediction overlap with EpiMap[45]. These analyses identified many biologically
436 plausible effectors genes.
437
438 Current weaknesses are the lack of population diversity in our GWAS dataset, as
439 these are comprised of associations only from European ancestry individuals.
440 Consequently, they will be missing population-specific findings, as have been
441 identified in other common diseases[62]. Furthermore, this lack of diversity is not only
442 limited to the genetic findings. The epigenomic maps, whilst being derived from a
443 breadth of cell-types giving good representation of strong tissue-specific regulatory
444 differences, are within each cell-type drawn from very small numbers. Therefore, they
445 lack detail regarding potential population variation in these functional units[63]. Another
446 weakness is that whilst benefitting from dense genotyping and imputation of common

SNVs, this is not exhaustive in capturing all the potential phenotypically associated genetic variation within each locus. This will miss the possible impact of rare SNVs, as well as any poorly tagged larger variants (copy number variants, short tandem repeats, inversions, *etc*.). Furthermore, these large variants may themselves facilitate functional epigenomic variation[64]. Future exploration of the phased interplay of genetic and epigenetic allelic elements by advancing long-read technologies will help to fill in these gaps[65].

In conclusion, we have identified plausible causal common genetic variants enriched in BP pathways. Their investigation through experimental biosystems will not only improve functional understanding of the biology of BP and its pathogenesis, but also potentially enable novel preventative and therapeutic opportunities.

Methods

Study data and detection of distinct association signals

We utilised previously reported GWAS meta-analyses of blood pressure traits in up to 757,601 individuals of European ancestry from the ICBP and UK Biobank[3] (ICBP+UKBB). Each contributing GWAS had been imputed up to reference panels from the 1000 Genomes Project [9,10] and/or Haplotype Reference Consortium[11]. After quality control, meta-analysis association summary statistics for SBP, DBP and PP were reported for 7,088,121, 7,160,657 and 7,088,842 SNVs, respectively. We began by considering autosomal lead SNVs that have been reported at genome-wide significance (variable threshold according to study design) for SBP, DBP or PP in previously published GWAS of blood pressure traits, which we have collated and are summarised in the recent review by Magavern and colleagues[8]. We initially defined genomic regions as mapping 500kb up- and down-stream of each lead SNV. However, where genomic regions overlapped, they were combined as a single genomic region to account for potential LD between previously reported lead SNVs. Genomic regions that did not attain genome-wide significance ($P < 5x10^{-8}$) in the ICBP+UKBB meta-analysis for any BP trait were not considered for downstream interrogation. We then performed approximate conditional analyses using GCTA-COJO[66] to detect distinct association signals at each genomic region for each BP trait separately, using European ancestry haplotypes from the 1000 Genomes Project (Phase 3, October 2014 release)[9] as a reference for LD. Within each genomic region variants attaining genome-wide significance ($P < 5x10^{-8}$) in the joint GCTA-COJO model were selected as index SNVs for distinct association signals.

We next assessed the evidence that distinct association signals for SBP, DBP and PP were shared across multiple BP traits. At each genomic region distinct association signals for two traits were considered to be the same if: (i) the index SNVs were the same for both traits; (ii) the index SNVs were colinear in the joint GCTA-COJO models for each trait after including the index SNV for the other trait in the model; or (iii) the P-value of the index SNV for one trait increased to $P > 0.05$ after including the index SNV for the other trait in the model, and the P-value of the index SNP for the other trait increased to $P > 0.0001$ for the corresponding reciprocal conditioning.

493 *Enrichment of BP associations for genomic annotations*

494 We used fGWAS[67] to identify genomic annotations enriched for SBP, DBP or PP
495 association signals. We considered a total of 253 functional and regulatory annotations
496 derived from: (i) genic regions (protein coding exons, 3' UTRs and 5' UTRs) as defined
497 by the GENCODE Project[13]; and (ii) chromatin state predictions of promoters and
498 enhancers across 125 tissues from the Roadmap Epigenome Consortium[15] via
499 Epilogos (http://compbio.mit.edu/epilogos/). For each BP trait separately, we used a
500 forward-selection approach to derive a joint model of enriched annotations. At each
501 iteration, we added the annotation to the joint fGWAS model that maximised the
502 improvement in the penalised likelihood. We continued until no additional annotations
503 improved the fit of the joint model (P<0.00020, Bonferroni correction for 253
504 annotations).
505
506 *Fine-mapping distinct association signals for BP traits*

507 For each trait, we began by approximating the Bayes' factor (BF), Λ_{ij}, in favour of
508 association of the jth SNV at the ith distinct association signal using summary
509 statistics from the ICBP+UKBB meta-analyses. Specifically,

510 $$\Lambda_{ij} = \exp\left[\frac{D_{ij} - lnK_{ij}}{2}\right],$$

511 where $D_{ij} = b_{ij}^2/v_{ij}$, and b_{ij} and v_{ij} are the allelic log-OR and corresponding variance,
512 respectively, across K_{ij} contributing GWAS to the ICBP+UKBB meta-analysis (here
513 $K_{ij} = 2$)[68]. At genomic regions with a single association signal, b_{ij} and v_{ij} were taken
514 from the unconditional meta-analysis. However, for genomic regions with multiple
515 association signals, b_{ij} and v_{ij} were taken from the joint GCTA-COJO model,
516 conditioning on the index SNVs for all other signals at the locus. The posterior
517 probability for the jth SNV at the ith distinct signal, was then given by $\pi_{ij} \propto \gamma_j \Lambda_{ij}$,
518 where γ_j is the relative prior probability of causality for the jth SNV. We considered an
519 annotation-informed prior model, for which

520 $$\gamma_j = \exp\left[\sum_k \hat{\beta}_k z_{jk}\right],$$

521 where the summation is over the enriched annotations, $\hat{\beta}_k$ is the estimated log-fold
522 enrichment of the kth annotation from the final joint fGWAS model, and z_{jk} is an
523 indicator variable taking the value 1 if the jth SNV maps to the kth annotation, and 0
524 otherwise. Finally, we derived a 99% credible set[69] for the ith distinct association

525 signal by: (i) ranking all SNVs according to their posterior probability π_{ij}; and (ii)
526 including ranked SNVs until their cumulative posterior probability attains or exceeds
527 0.99.
528
529 *High Confidence SNV Gene Set Enrichment Analysis*
530 Genomic Regions Enrichment of Annotations Tool (GREAT) v4.0.4[16] was used to
531 explore the high confidence SNVs potential biological impact. The default GREAT
532 association parameters for gene regulatory domains (Proximal 5 kb upstream, 1 kb
533 downstream, plus Distal up to 1 Mb) were used and curated regulatory domains
534 included. Input was SNV BED files for each of the three traits (SBP n = 208, DBP n =
535 224 and PP n = 158). GREAT analysis included gene ontology (GO) Biological
536 Processes, Human Phenotype, Mouse Phenotype and Knockout data.
537
538 *Functional annotation*
539 We use Variant-effect predictor (VEP) analysis to identify missense variants and
540 queried their overlap with high confidence causal variants from the credible set
541 analysis (https://grch37.ensembl.org/Homo_sapiens/Tools/VEP)[70].
542
543 *Transcription Factor Binding Motif Analysis*
544 We used the Transcription Factor Affinity Prediction (TRAP) v3.0.5[71] multiple
545 sequences option to explore any enrichment for Transcription Factor (TF) binding
546 motifs within the high confidence non-coding variants for each of the three traits (SBP
547 n= 178; DBP n=187; and PP n =137). Sequences around each non-coding SNV were
548 expanded to +/-10bp (via AWK) and the FASTA sequence extracted (hg19) via the
549 BEDtools v2.30.0 command getfasta[72]. The Transfac 2010.1 Vertebrate matrix set
550 was interrogated with human_promoter set as background model and the results were
551 required to pass a Benjamini-Hochberg multiple-testing correction.
552
553 *Colocalization with gene expression data*
554 We performed a Bayesian statistical procedure to assess whether our annotation
555 informed GWAS results were colocalised with eQTL results. We used all available
556 eQTL tissues relevant for blood pressure (adipose, adrenal gland, artery, kidney
557 cortex, heart, nerve, and brain) from the publicly available eQTL results from GTEx

558 version 8[24]. The annotation informed BF in favour of association of the jth SNV at the
559 ith distinct association signal was defined as:

560 $$\Lambda_{ij} = \pi_{ij} \sum_{j} \Lambda_{ij}$$

561 In this expression, π_{ij} is the annotation-informed posterior probability, and Λ_{ij} is the
562 BF defined above. GWAS results were lifted from hg19 to hg38 used lift Over
563 software[73] [to allow direct comparison with the hg38 eQTL data. We undertook
564 colocalization using the annotation informed BF using the COLOC software package
565 in R[74], only for those signals for which a 99% credible set variant was the lead eQTL
566 SNV**.**
567
568 *Long-range chromatin interaction (Hi–C) analyses*
569 We identified potential target genes of regulatory SNVs using long-range chromatin
570 interaction (Hi–C) data from tissues and cell types relevant for blood pressure
571 regulation (adrenal gland, left and right ventricles, hippocampus, and cortex)[42]. Hi–C
572 data is corrected for genomic biases and distance using the Hi–C Pro and Fit-Hi-C
573 pipelines according to Schmitt et al. (40 kb resolution—correction applied to
574 interactions with 50 kb- 5Mb span)[75]. We selected the most significant promoter
575 interactions for all potential regulatory SNPs (RegulomeDB score ≤3) that were
576 included in the 99% credible sets and report the interactors with the SNPs of highest
577 regulatory potential to annotate the loci.
578
579 *Collation of evidence for effector BP genes*
580 A full list of candidate effector genes for each BP trait was collated from the results of
581 our fine-mapping pipeline and computational approaches. A gene was indicated for a
582 signal if there was support from a coding and high confidence variant in the gene at
583 the locus, or if the gene was indicated from eQTL colocalization or Hi-C analyses. To
584 refine the list of putative candidate effector genes we next collated additional
585 information for each gene using data from GeneCards
586 (https://genealacart.genecards.org). This included the following: 1) a mouse model
587 from Mouse Genome Informatics (MGI) which has a cardiovascular or renal
588 phenotype. 2) A cardiovascular, vascular or renal phenotype described for the
589 candidate gene in the Human Phenotype Ontology database 3) Differential RNA

expression of the candidate gene in the GTEx database in cardiovascular, vascular or renal tissues, only genes with fold changes >4 in a tissue were selected. 4) Differential protein expression of the candidate gene based on 69 integrated normal proteomics datasets in HIPED (the Human Integrated Protein Expression Database). Genes with a fold change value of >6 and protein abundance value of >0.1 PPM in an anatomical were selected. The top effector candidate genes for each BP trait were selected if there were at least 2 additional lines of evidence.

Effector gene pathway analysis

We used the Gene2Function analysis tool in FUMA (v1.4.0) to perform geneset enrichment and identify significantly associated GO terms and pathways[76]. Hypergeometric tests were performed to test if genes were over-represented in any predefined gene set and multiple testing correction was performed per category. The gene sets used are from MsigDB, WikiPathways and genes from the GWAS-catalog. The analysis included the putative top effector genes only. The analysis was done for all BP traits and we report results with adjusted p-values of <0.05. Redundant GO terms were removed using the Reduce and Visualize Gene Ontology (REVIGO) web application[77]. REVIGO uses a hierarchical clustering method to remove highly similar terms, incorporating enrichment *P*-values in the selection process. Default settings (dispensability cut off <0.7) were used in this analysis.

Druggability of prioritised effector genes

To identify candidate druggable targets, a look-up was performed in a previously published database of the druggable genome developed by Finan et al.[53] This list contains protein-coding genes catagorised into three tiers: Tier 1 are targets of approved drugs and some drugs in clinical development, including targets of small molecules and biotherapeutics; Tier 2 are proteins closely related to drug targets or associated with drug-like compounds (≥50% shared protein sequence identity); Tier 3 includes extracellular proteins and members of key drug target families in Tier 1 (e.g., G protein-coupled receptors). To identify potential opportunities for drug repurposing, a look-up of each BP candidate gene was performed in Tier 1 to identify existing drug targets (https://www.genome.jp/kegg/genes.html). Primary targets of antihypertensives were also identified using the KEGG drug database (https://www.genome.jp/kegg/drug/). The open targets database was subsequently

624 interrogated to identify disease associations with each gene, to identify potential
625 overlap that could indicate promising drug targets. Target, drug and disease
626 association data was downloaded from the platform
627 (https://platform.opentargets.org/downloads). Open targets calculates association
628 scores to capture the data type (e.g., gene level) and source, to aggregate evidence
629 for an association, by calculating the harmonic sum using a weighted vector of data
630 source scores. This sum is divided by the maximum theoretical value, resulting in a
631 score between 0 and 1. To identify enrichment of candidate effector genes in clinical
632 indication categories and potentially re-positional drugs, we utilised the Genome for
633 REPositioning drugs (GREP) software[78]. GREP performs a series of Fisher's exact
634 tests, to identify enrichment of a gene-set in genes targeted by a drug in a clinical
635 indication category (Anatomical Therapeutic Chemical Classification System [ATC] or
636 International Classification of Diseases 10 [ICD10] diagnostic codes).
637
638
639

Figure Legends

Figure 1. Overlap of 1,850 distinct signals attaining genome-wide significant evidence of association with SBP, DBP and PP in meta-analysis of BP GWAS in up to 757,601 individuals of European ancestry.

(a) Venn diagram showing the number of signals shared across BP traits. Sharing of signals across traits is much more common between SBP and DBP or SBP and PP, with just 16 associations shared between only DBP and PP. (b) Comparison of allelic effect sizes on SBP, DBP and PP for the index SNV at the 532 distinct association signals that are shared across multiple BP traits. The effect has been aligned to the SBP or PP increasing allele for the signal. Blue points correspond to the 448 association signals that are shared across exactly two BP traits, whilst red points correspond to the 84 association signals that are shared across all three BP traits. When signals are shared between SBP and PP, the direction of effect of the index SNV on the traits is always concordant.

Figure 2. Distinct BP association signals.

(a) Summary of distinct association signals for blood pressure traits. SBP: A single signal at 277 genomic regions and at least two at 180; DBP: A single signal at 262 genomic regions, and at least two at 188; PP: A single signal at 265 genomic regions, and at least two at 144. (b) Distribution of the posterior probability of causality of the variants in credible sets. SBP, systolic blood pressure; DBP, diastolic blood pressure; PP, pulse pressure.

Figure. 3. Colocalization between GWAS signals for systolic blood pressure and multi-tissue expression data at locus ID 580 on chromosome 17.

The top panel shows the unconditional GWAS data of the genomic region at chromosome 17 (60.2Mb – 62.9Mb) for systolic blood pressure. The lower four panels show the log annotation informed Bayesian factors of the conditional GWAS signal (blue, left axis) and gene expression data from GTeX eQTL data (red, right axis). Three distinct annotation informed signals colocalized with gene expression data from: *MRC2* (second panel) in tibial artery tissue, *ACE* (third panel) in kidney cortex tissue, and *CEP95* and *DDX5* in aortic artery tissue (bottom panels).

673 The x-axis shows the physical position on the chromosome (Mb) and the y-axes show
674 the log annotation informed Bayesian factor from the GWAS (left axis) and the gene
675 expression data (right axis). The intensity of the color indicates the linkage
676 disequilibrium with respect to the sentinel GWAS SNP (blue) or top eQTL SNP (red).
677
678 **Figure 4. BP fine mapping results and consolidated effector genes.**
679 Overview of results from the fine-mapping pipeline for SBP, DBP and PP. For each
680 trait the number of signals are shown following annotation as missense, eQTL or
681 regulatory, and the number of candidate effector genes based on at least one line of
682 evidence. Using additional evidence from mouse models, human cardiovascular and
683 renal phenotypes and gene/protein expression the list of effector genes was reduced
684 – these are the consolidated effector genes. The consolidated effector genes were
685 used as input to FUMA (methods) for pathway enrichment analysis. Results are
686 shown for GO terms after removal of similar terms using the Reduce and Visualise
687 Gene Ontology (REVIGO) web application (dispensibility cut off <0.3), and only
688 pathways which had adjusted *P* values $<10^{-10}$ were included. Created with
689 Biorender.com

References

1. Forouzanfar, M.H. *et al.* Global Burden of Hypertension and Systolic Blood Pressure of at Least 110 to 115 mm Hg, 1990-2015. *JAMA* **317**, 165-182 (2017).
2. G. B. D. Risk Factors Collaborators. Global burden of 87 risk factors in 204 countries and territories, 1990-2019: a systematic analysis for the Global Burden of Disease Study 2019. *Lancet* **396**, 1223-1249 (2020).
3. Evangelou, E. *et al.* Genetic analysis of over 1 million people identifies 535 new loci associated with blood pressure traits. *Nat Genet* **50**, 1412-1425 (2018).
4. Giri, A. *et al.* Trans-ethnic association study of blood pressure determinants in over 750,000 individuals. *Nat Genet* **51**, 51-62 (2019).
5. Sakaue, S. *et al.* A cross-population atlas of genetic associations for 220 human phenotypes. *Nat Genet* **53**, 1415-1424 (2021).
6. Ehret, G.B. *et al.* The genetics of blood pressure regulation and its target organs from association studies in 342,415 individuals. *Nat Genet* **48**, 1171-1184 (2016).
7. Surendran, P. *et al.* Discovery of rare variants associated with blood pressure regulation through meta-analysis of 1.3 million individuals. *Nat Genet* **52**, 1314-1332 (2020).
8. Magavern, E.F. *et al.* An Academic Clinician's Road Map to Hypertension Genomics: Recent Advances and Future Directions MMXX. *Hypertension* **77**, 284-295 (2021).
9. The 1000 Genomes Project Consortium *et al.* An integrated map of genetic variation from 1,092 human genomes. *Nature* **491**, 56-65 (2012).
10. The 1000 Genomes Project Consortium. A global reference for human genetic variation. *Nature* **526**, 68-74 (2015).
11. McCarthy, S. *et al.* A reference panel of 64,976 haplotypes for genotype imputation. *Nat Genet* **advance online publication**(2016).
12. Schaid, D.J., Chen, W. & Larson, N.B. From genome-wide associations to candidate causal variants by statistical fine-mapping. *Nat Rev Genet* **19**, 491-504 (2018).
13. Harrow, J. *et al.* GENCODE: the reference human genome annotation for The ENCODE Project. *Genome Res.* **22**(2012).
14. Bernstein, B.E. *et al.* An integrated encyclopedia of DNA elements in the human genome. *Nature* **489**, 57-74 (2012).
15. Roadmap Epigenomics Consortium *et al.* Integrative analysis of 111 reference human epigenomes. *Nature* **518**, 317-330 (2015).
16. McLean, C.Y. *et al.* GREAT improves functional interpretation of cis-regulatory regions. *Nature biotechnology* **28**, 495-501 (2010).
17. Milman, N.T., Schioedt, F.V., Junker, A.E. & Magnussen, K. Diagnosis and Treatment of Genetic HFE-Hemochromatosis: The Danish Aspect. *Gastroenterology Res* **12**, 221-232 (2019).
18. Sounni, N.E. *et al.* Stromal regulation of vessel stability by MMP14 and TGFbeta. *Dis Model Mech* **3**, 317-32 (2010).
19. Wu, J. *et al.* Aortic constriction induces hypertension and cardiac hypertrophy via (pro)renin receptor activation and the PLC-beta3 signaling pathway. *Mol Med Rep* **19**, 573-580 (2019).

20. Merkulova, M. *et al.* Targeted deletion of the Ncoa7 gene results in incomplete distal renal tubular acidosis in mice. *Am J Physiol Renal Physiol* **315**, F173-F185 (2018).
21. Mohney, B.G. *et al.* A novel mutation of LAMB2 in a multigenerational mennonite family reveals a new phenotypic variant of Pierson syndrome. *Ophthalmology* **118**, 1137-44 (2011).
22. Larionov, A. *et al.* Cathepsin B increases ENaC activity leading to hypertension early in nephrotic syndrome. *J Cell Mol Med* **23**, 6543-6553 (2019).
23. Bower, M. *et al.* Update of PAX2 mutations in renal coloboma syndrome and establishment of a locus-specific database. *Hum Mutat* **33**, 457-66 (2012).
24. GTEx Consortium. The GTEx Consortium atlas of genetic regulatory effects across human tissues. *Science* **369**, 1318-1330 (2020).
25. Xu, Y., Rong, J. & Zhang, Z. The emerging role of angiotensinogen in cardiovascular diseases. *J Cell Physiol* **236**, 68-78 (2021).
26. Carney, E.F. Hypertension: Role of ARHGAP42 in hypertension. *Nat Rev Nephrol* **13**, 134 (2017).
27. Koscielny, G. *et al.* The International Mouse Phenotyping Consortium Web Portal, a unified point of access for knockout mice and related phenotyping data. *Nucleic Acids Res* **42**, D802-9 (2014).
28. Tsukahara, H., Gordienko, D.V., Tonshoff, B., Gelato, M.C. & Goligorsky, M.S. Direct demonstration of insulin-like growth factor-I-induced nitric oxide production by endothelial cells. *Kidney Int* **45**, 598-604 (1994).
29. Karamanavi, E. *et al.* The FES Gene at the 15q26 Coronary-Artery-Disease Locus Inhibits Atherosclerosis. *Circ Res* **131**, 1004-1017 (2022).
30. Seo, H.-R. *et al.* Intrinsic FGF2 and FGF5 promotes angiogenesis of human aortic endothelial cells in 3D microfluidic angiogenesis system. *Scientific Reports* **6**, 28832 (2016).
31. Reynolds, J.O. *et al.* Junctophilin-2 gene therapy rescues heart failure by normalizing RyR2-mediated Ca2+ release. *International Journal of Cardiology* **225**, 371-380 (2016).
32. Collin, T. *et al.* Cloning, chromosomal location and functional expression of the human voltage-dependent calcium-channel beta 3 subunit. *Eur J Biochem* **220**, 257-62 (1994).
33. Bult, C.J. *et al.* Mouse Genome Database (MGD) 2019. *Nucleic Acids Res* **47**, D801-D806 (2019).
34. Newton-Cheh, C. *et al.* Genome-wide association study identifies eight loci associated with blood pressure. *Nat Genet* **41**, 666-76 (2009).
35. International Consortium for Blood Pressure Genome-Wide Association, S. *et al.* Genetic variants in novel pathways influence blood pressure and cardiovascular disease risk. *Nature* **478**, 103-9 (2011).
36. Rappaport, N. *et al.* MalaCards: an amalgamated human disease compendium with diverse clinical and genetic annotation and structured search. *Nucleic Acids Res* **45**, D877-D887 (2017).
37. Wilson, M.P., Plecko, B., Mills, P.B. & Clayton, P.T. Disorders affecting vitamin B(6) metabolism. *J Inherit Metab Dis* **42**, 629-646 (2019).
38. Wienke, D. *et al.* The collagen receptor Endo180 (CD280) Is expressed on basal-like breast tumor cells and promotes tumor growth in vivo. *Cancer Res* **67**, 10230-40 (2007).
39. Imig, J.D. ACE Inhibition and Bradykinin-Mediated Renal Vascular Responses: EDHF Involvement. *Hypertension* **43**, 533-5 (2004).

40. Fan, Y. *et al.* Protective Role of RNA Helicase DEAD-Box Protein 5 in Smooth Muscle Cell Proliferation and Vascular Remodeling. *Circ Res* **124**, e84-e100 (2019).
41. Seda, O. *et al.* Connexin 50 mutation lowers blood pressure in spontaneously hypertensive rat. *Physiol Res* **66**, 15-28 (2017).
42. Jung, I. *et al.* A compendium of promoter-centered long-range chromatin interactions in the human genome. *Nat Genet* **51**, 1442-1449 (2019).
43. Chao, J., Jin, L., Lin, K.F. & Chao, L. Adrenomedullin gene delivery reduces blood pressure in spontaneously hypertensive rats. *Hypertens Res* **20**, 269-77 (1997).
44. Yan, Y., Liu, F., Dang, X., Zhou, R. & Liao, B. TBX3 induces biased differentiation of human induced pluripotent stem cells into cardiac pacemaker-like cells. *Gene Expr Patterns* **40**, 119184 (2021).
45. Boix, C.A., James, B.T., Park, Y.P., Meuleman, W. & Kellis, M. Regulatory genomic circuitry of human disease loci by integrative epigenomics. *Nature* **590**, 300-307 (2021).
46. Warren, H.R. *et al.* Genome-wide association analysis identifies novel blood pressure loci and offers biological insights into cardiovascular risk. *Nat Genet* **49**, 403-415 (2017).
47. Huo, Y. *et al.* Efficacy of folic acid therapy in primary prevention of stroke among adults with hypertension in China: the CSPPT randomized clinical trial. *JAMA* **313**, 1325-35 (2015).
48. Perala, N. *et al.* Sema4C-Plexin B2 signalling modulates ureteric branching in developing kidney. *Differentiation* **81**, 81-91 (2011).
49. Zhu, L. *et al.* Mutations in myosin heavy chain 11 cause a syndrome associating thoracic aortic aneurysm/aortic dissection and patent ductus arteriosus. *Nat Genet* **38**, 343-9 (2006).
50. Kuang, S.Q. *et al.* Rare, nonsynonymous variant in the smooth muscle-specific isoform of myosin heavy chain, MYH11, R247C, alters force generation in the aorta and phenotype of smooth muscle cells. *Circ Res* **110**, 1411-22 (2012).
51. Klewer, S.E., Krob, S.L., Kolker, S.J. & Kitten, G.T. Expression of type VI collagen in the developing mouse heart. *Dev Dyn* **211**, 248-55 (1998).
52. Zech, M. *et al.* Recessive mutations in the alpha3 (VI) collagen gene COL6A3 cause early-onset isolated dystonia. *Am J Hum Genet* **96**, 883-93 (2015).
53. Finan, C. *et al.* The druggable genome and support for target identification and validation in drug development. *Sci Transl Med* **9**(2017).
54. El-Bassossy, H., Badawy, D., Neamatallah, T. & Fahmy, A. Ferulic acid, a natural polyphenol, alleviates insulin resistance and hypertension in fructose fed rats: Effect on endothelial-dependent relaxation. *Chem Biol Interact* **254**, 191-7 (2016).
55. Maass, P.G. *et al.* PDE3A mutations cause autosomal dominant hypertension with brachydactyly. *Nat Genet* **47**, 647-53 (2015).
56. Ercu, M. *et al.* Mutant Phosphodiesterase 3A Protects From Hypertension-Induced Cardiac Damage. *Circulation* **146**, 1758-1778 (2022).
57. Jain, A.P. *et al.* MAP2K1 is a potential therapeutic target in erlotinib resistant head and neck squamous cell carcinoma. *Sci Rep* **9**, 18793 (2019).
58. Olzinski, A.R. *et al.* Hypertensive target organ damage is attenuated by a p38 MAPK inhibitor: role of systemic blood pressure and endothelial protection. *Cardiovasc Res* **66**, 170-8 (2005).

59. Eales, J.M. *et al.* Uncovering genetic mechanisms of hypertension through multi-omic analysis of the kidney. *Nat Genet* **53**, 630-637 (2021).
60. Gazal, S. *et al.* Combining SNP-to-gene linking strategies to identify disease genes and assess disease omnigenicity. *Nat Genet* **54**, 827-836 (2022).
61. Boix, C.A., James, B.T., Park, Y.P., Meuleman, W. & Kellis, M. Regulatory genomic circuitry of human disease loci by integrative epigenomics. *Nature* (2021).
62. Washington, C., 3rd *et al.* African-specific alleles modify risk for asthma at the 17q12-q21 locus in African Americans. *Genome Med* **14**, 112 (2022).
63. Breeze, C.E., Beck, S., Berndt, S.I. & Franceschini, N. The missing diversity in human epigenomic studies. *Nat Genet* **54**, 737-739 (2022).
64. Bell, C.G. *et al.* Obligatory and facilitative allelic variation in the DNA methylome within common disease-associated loci. *Nature Communications* **9**, 8 (2018).
65. Battaglia, S. *et al.* Long-range phasing of dynamic, tissue-specific and allele-specific regulatory elements. *Nat Genet* **54**, 1504-1513 (2022).
66. Yang, J. *et al.* Conditional and joint multiple-SNP analysis of GWAS summary statistics identifies additional variants influencing complex traits. *Nat Genet* **44**, 369-75, S1-3 (2012).
67. Pickrell, J.K. Joint analysis of functional genomic data and genome-wide association studies of 18 human traits. *Am J Hum Genet* **94**, 559-73 (2014).
68. Kass, R.E. & Raftery, A.E. Bayes Factors. *Journal of the American Statistical Association* **90**, 773-795 (1995).
69. Maller, J.B. *et al.* Bayesian refinement of association signals for 14 loci in 3 common diseases. *Nature Genetics* **44**, 1294-1301 (2012).
70. McLaren, W. *et al.* Deriving the consequences of genomic variants with the Ensembl API and SNP Effect Predictor. *Bioinformatics* **26**, 2069-70 (2010).
71. Thomas-Chollier, M. *et al.* Transcription factor binding predictions using TRAP for the analysis of ChIP-seq data and regulatory SNPs. *Nat Protoc* **6**, 1860-9 (2011).
72. Quinlan, A.R. & Hall, I.M. BEDTools: a flexible suite of utilities for comparing genomic features. *Bioinformatics* **26**, 841-2 (2010).
73. Hinrichs, A.S. *et al.* The UCSC Genome Browser Database: update 2006. *Nucleic Acids Res* **34**, D590-8 (2006).
74. Giambartolomei, C. *et al.* Bayesian test for colocalisation between pairs of genetic association studies using summary statistics. *PLoS Genet* **10**, e1004383 (2014).
75. Schmitt, A.D. *et al.* A Compendium of Chromatin Contact Maps Reveals Spatially Active Regions in the Human Genome. *Cell Rep* **17**, 2042-2059 (2016).
76. Watanabe, K., Taskesen, E., van Bochoven, A. & Posthuma, D. Functional mapping and annotation of genetic associations with FUMA. *Nat Commun* **8**, 1826 (2017).
77. Supek, F., Bosnjak, M., Skunca, N. & Smuc, T. REVIGO summarizes and visualizes long lists of gene ontology terms. *PLoS One* **6**, e21800 (2011).
78. Sakaue, S. & Okada, Y. GREP: genome for REPositioning drugs. *Bioinformatics* **35**, 3821-3823 (2019).

Acknowledgements

This research was supported by the NIHR Barts Cardiovascular Research Centre and the NIHR Manchester Biomedical Research Centre (NIHR203308). J.R. acknowledges funding from the European Union's Horizon 2020 Research and Innovation Programme under the Marie Sklodowska-Curie grant agreement number 786833, from the European Union-NextGenerationEU, and from Grant PID2021-128972OA-I00 funded by MCIN/AEI/ 10.13039/501100011033. W.J.Y. recognises the National Institute for Health Research (NIHR) Integrated Academic Training programme, which supports his Academic Clinical Lectureship post.

Ethics declarations

The authors declare no competing interests.

Author Contributions

S.vD., J.R., W.J.Y., C.G.B., A.P.M., P.B.M designed the study. S.vD., J.R., W.J.Y., K.J.O., F.A., M.J.A.Y.A., C.G.B.., A.P.M., P.B.M. performed analyses. S.vD., J.R., W.J.Y., C.G.B., A.P.M., P.B.M. drafted the manuscript, and all authors provided critical revisions.

Table 1| High-confidence missense variants for blood pressure association signals

Signal ID	Index SNV	Missense variant	Canonical transcript	Annotation	Chr	Position	Polyphen	SIFT	Trait	p-value	Posterior probability (%)
1_6	rs262695	rs262695	ENST00000545087.1	*AL590822.1* p.Cys78Arg	1	2,144,788	N/A	N/A	SBP	9.4E-14	96.2
									PP	1.6E-12	99.1
3_1	rs11121483	rs846111	ENST00000377939.4	*RNF207* p.Gly603Ala	1	6,279,370	benign	tolerated (LC)	PP	1.8E-10	83.5
39_1	rs150816167	rs61747728	ENST00000367615.4	*NPHS2* p.Arg229Gln	1	179,526,214	possibly damaging	tolerated	DBP	5.7E-11	88.1
52_1	rs699	rs699	ENST00000366667.4	*AGT* p.Met268Thr	1	230,845,794	benign	tolerated	SBP	5.6E-34	93.6
60_2	rs2384061	rs11676272	ENST00000260600.5	*ADCY3* p.Ser107Pro	2	25,141,538	benign	tolerated	DBP	5.4E-23	86.8
98_5	rs10497529	rs10497529	ENST00000420890.2	*CCDC141* p.Ala141Val	2	179,839,888	probably damaging	deleterious	PP	8.1E-18	89.0
108_1	rs1047891	rs1047891	ENST00000430249.2	*CPS1* p.Thr1412Asn	2	211,540,507	benign	tolerated	SBP	1.4E-14	98.5
									DBP	8.2E-14	99.5
110_1	rs1250259	rs1250259	ENST00000354785.4	*FN1* p.Gln15Leu	2	216,300,482	benign	tolerated	SBP	7.5E-20	92.3
									PP	8.6E-33	86.1
132_2	rs74951356	rs74951356	ENST00000418109.1	*LAMB2* p.Ala1765Thr	3	49,158,763	benign	tolerated	DBP	5.0E-09	95.8
135_1	rs3772219	rs3772219	ENST00000338458.4	*ARHGEF3* p.Leu367Val	3	56,771,251	benign	tolerated	SBP	3.1E-17	75.2
									DBP	1.7E-24	81.1
158_3	rs61762319	rs61762319	ENST00000460393.1	*MME* p.Met8Val	3	154,801,978	benign	deleterious	SBP	1.5E-09	99.8
170_6	rs2498323	rs2498323	ENST00000382774.3	*HGFAC* p.Arg644Gln	4	3,451,109	possibly damaging	tolerated	PP	7.4E-13	100.0
174_1	rs2302212	rs2302212	ENST00000514176.1	*NCAPG* p.Met231Thr	4	17,818,885	benign	deleterious	SBP	4.1E-08	84.2

191_3	rs13107325	rs13107325	ENST00000394833.2	*SLC39A8* p.Ala391Thr	4	103,188,709	possibly damaging	tolerated	SBP	4.2E-53	100.0
									DBP	2.5E-90	100.0
221_1	rs2307111	rs2307111	ENST00000428202.2	*POC5* p.His36Arg	5	75,003,678	benign	tolerated	DBP	1.6E-22	97.6
237_6	rs12189018	rs1042713	ENST00000305988.4	*ADRB2* p.Gly16Arg	5	148,206,440	benign	tolerated	DBP	8.1E-09	81.7
237_7	rs1800888	rs1800888	ENST00000305988.4	*ADRB2* p.Thr164Ile	5	148,206,885	benign	tolerated	DBP	7.4E-13	100.0
249_4	rs198851	rs1799945	ENST00000357618.5	*HFE* p.His63Asp	6	26,091,179	probably damaging	tolerated	DBP	5.7E-51	85.3
249_1	rs1800730	rs1800730	ENST00000357618.5	*HFE* p.Ser65Cys	6	26,091,185	probably damaging	deleterious	SBP	2.0E-09	96.4
									DBP	1.6E-18	100.0
249_3	rs1800562	rs1800562	ENST00000357618.5	*HFE* p.Cys282Tyr	6	26,093,141	probably damaging	deleterious	SBP	2.0E-14	89.1
									DBP	2.1E-37	96.4
251_7	rs41543814	rs41543814	ENST00000376228.5	*HLA-C* p.Ala97Thr	6	31,239,430	benign	tolerated (LC)	DBP	1.5E-19	100.0
251_10	rs2844573	rs2308655	ENST00000412585.2	*HLA-B* p.Cys349Ser	6	31,322,303	benign	tolerated (LC)	PP	1.4E-12	99.2
251_11	rs1077393	rs1052486	ENST00000375964.6	*BAG6* p.Ser625Pro	6	31,610,686	benign	tolerated	DBP	4.6E-24	86.1
252_1	rs3176336	rs2395655	ENST00000448526.2	*CDKN1A* p.Asp28Gly	6	36,645,696	benign	tolerated (LC)	PP	4.7E-13	98.5
255_1	rs78648104	rs78648104	ENST00000008391.3	*TFAP2D* p.Phe74Leu	6	50,683,009	benign	tolerated	SBP	2.4E-15	99.9
									DBP	2.9E-20	100.0
272_1	rs6919947	rs6919947	ENST00000368357.3	*NCOA7* p.Ser399Ala	6	126,210,395	benign	tolerated (LC)	SBP	4.9E-17	100.0
									DBP	2.2E-13	99.9
300_2	rs2107732	rs2107732	ENST00000381112.3	*CCM2* p.Val74Ile	7	45,077,978	benign	tolerated	DBP	3.3E-10	80.6
300_3	rs2854746	rs2854746	ENST00000381083.4	*IGFBP3* p.Ala32Gly	7	45,960,645	benign	tolerated	DBP	5.0E-11	97.9

313_2	rs11556924	rs11556924	ENST00000358303.4	*ZC3HC1* p.Arg363His	7	129,663,496	probably damaging	deleterious	DBP	1.5E-26	98.3
313_4	rs13222308	rs3734928	ENST00000335420.5	*KLHDC10* p.Ser2Leu	7	129,710,488	benign	deleterious (LC)	SBP	1.3E-10	90.0
353_10	rs34591516	rs34591516	ENST00000377741.3	*GPR20* p.Gly313Ser	8	142,367,087	benign	tolerated	DBP	1.3E-15	80.8
365_2	rs76452347	rs76452347	ENST00000354323.2	*HRCT1* p.Arg63Trp	9	35,906,471	possibly damaging	deleterious (LC)	SBP	7.1E-14	100.0
									DBP	8.0E-23	100.0
372_3	rs3739451	rs3739451	ENST00000401783.2	*SVEP1* p.Phe3161Ile	9	113,166,792	benign	N/A	SBP	9.5E-11	84.7
379_2	rs6271	rs6271	ENST00000393056.2	*DBH* p.Arg549Cys	9	136,522,274	possibly damaging	tolerated	SBP	1.2E-19	97.6
									DBP	5.7E-35	100.0
394_1	rs2236295	rs2236295	ENST00000373783.1	*ADO* p.Gly25Trp	10	64,564,892	possibly damaging	tolerated	SBP	2.8E-22	96.7
									DBP	1.0E-28	89.4
402_3	rs2274224	rs2274224	ENST00000371380.3	*PLCE1* p.Arg1575Pro	10	96,039,597	benign	tolerated	SBP	9.0E-57	96.6
									DBP	3.2E-44	93.4
406_5	rs2484294	rs1801253	ENST00000369295.2	*ADRB1* p.Gly389Arg	10	115,805,056	benign	tolerated	DBP	2.3E-74	89.3
412_3	rs1133400	rs1133400	ENST00000368594.3	*INPP5A* p.Lys45Arg	10	134,459,388	benign	tolerated	SBP	5.0E-15	77.8
									PP	3.0E-10	86.1
414_7	rs686722	rs686722	ENST00000418975.1	*LSP1* p.Arg12Trp	11	1,891,722	N/A	N/A	PP	8.1E-19	82.6
417_10	rs10770059 (SBP) rs415895 (DBP)	rs415895	ENST00000318950.6	*SWAP70* p.Gln505Glu	11	9,769,562	benign	tolerated	SBP	5.0E-47	96.5
									DBP	3.3E-69	96.8
432_4	rs117874826	rs117874826	ENST00000540288.1	*PLCB3* p.Glu564Ala	11	64,027,666	benign	deleterious	SBP	2.3E-11	100.0
434_1	rs36027301	rs36027301	ENST00000265686.3	*TCIRG1* p.Arg56Trp	11	67,809,268	probably damaging	deleterious	SBP	6.0E-11	97.6

									DBP	6.4E-12	77.8
447_7	rs573455	rs573455	ENST00000278935.3	*CEP164* p.Gln1119Arg	11	117,267,884	benign	tolerated	PP	8.7E-34	100.0
463_15	rs1126930	rs1126930	ENST00000316299.5	*PRKAG1* p.Thr98Ser	12	49,399,132	benign	tolerated	PP	4.6E-14	95.6
499_1	rs17880989	rs17880989	ENST00000311852.6	*MMP14* p.Met355Ile	14	23,313,633	benign	deleterious	DBP	3.2E-12	100.0
499_4	rs365990	rs365990	ENST00000405093.3	*MYH6* p.Val1101Ala	14	23,861,811	benign	tolerated	SBP	2.2E-12	90.8
523_5	rs11854184	rs11854184	ENST00000559471.1	*SECISBP2L* p.Val710Leu	15	49,293,194	benign	tolerated	DBP	2.3E-10	86.8
549_2	rs55861648	rs62622830	ENST00000541260.1	*C16orf93* p.Lys189Glu	16	30,770,950	N/A	tolerated	PP	1.2E-09	82.7
558_2	rs62051555	rs62051555	ENST00000268489.5	*ZFHX3* p.Gln2014His	16	72,830,539	probably damaging	N/A	PP	5.1E-25	89.9
571_4	rs1043809	rs4924987	ENST00000477478.2	*B9D1* p.His143Tyr	17	19,247,075	benign	tolerated (LC)	DBP	1.8E-16	77.2
572_1	rs704	rs704	ENST00000226218.4	*VTN* p.Thr400Met	17	26,694,861	benign	tolerated	SBP	1.9E-08	96.5
573_1	rs11080134 (SBP) rs9894838 (DBP)	rs11080134	ENST00000321990.4	*ATAD5* p.Glu135Gly	17	29,161,503	benign	deleterious	SBP	1.8E-08	91.4
									DBP	2.2E-08	79.5
576_26	rs7406910 (SBP) rs9221 (PP)	rs7406910	ENST00000239165.7	*HOXB7* p.Thr9Ala	17	46,688,256	benign	tolerated	SBP	1.1E-17	79.5
									PP	5.1E-25	96.3
582_6	rs34587622	rs34587622	ENST00000427177.1	*SEPT9* p.Pro145Leu	17	75,398,498	benign	tolerated (LC)	SBP	6.2E-14	99.9
592_1	rs61735998	rs61735998	ENST00000257209.4	*FHOD3* p.Val647Phe	18	34,289,285	benign	deleterious (LC)	PP	2.0E-11	87.8
606_7	rs35918208	rs2291516	ENST00000393423.3	*RGL3* p.Arg621Cys	19	11,508,177	N/A	tolerated	DBP	9.4E-11	85.7
606_9	rs167479	rs167479	ENST00000393423.3	*RGL3* p.Pro162His	19	11,526,765	probably damaging	deleterious	SBP	8.7E-69	100.0
									DBP	2.4E-79	100.0

									PP	9.4E-21	100.0
608_1	rs2108622	rs2108622	ENST00000221700.6	*CYP4F2* p.Val433Met	19	15,990,431	probably damaging	deleterious	DBP	1.1E-08	83.0
608_2	rs4808045	rs3745318	ENST00000248071.5	*KLF2* p.Leu104Pro	19	16,436,262	benign	tolerated	DBP	3.0E-14	89.1
610_2	rs45522544	rs45522544	ENST00000357324.6	*ATP13A1* p.Glu556Lys	19	19,765,499	benign	tolerated	DBP	3.1E-08	100.0
616_4	rs34093919	rs34093919	ENST00000308370.7	*LTBP4* p.Asp752Asn	19	41,117,300	possibly damaging	deleterious	PP	2.8E-14	97.4
616_7	rs1800470	rs1800470	ENST00000221930.5	*TGFB1* p.Pro10Leu	19	41,858,921	N/A	tolerated (LC)	PP	1.9E-15	99.0
617_2	rs7412	rs7412	ENST00000252486.4	*APOE* p.Arg176Cys	19	45,412,079	probably damaging	deleterious	SBP	2.0E-14	100.0
									PP	2.8E-20	99.4
623_3	rs35761929	rs35761929	ENST00000254958.5	*JAG1* p.Pro871Arg	20	10,622,501	benign	deleterious	DBP	2.6E-18	99.1
636_1	rs2229742	rs2229742	ENST00000400202.1	*NRIP1* p.Arg448Gly	21	16,339,172	probably damaging	deleterious	SBP	7.4E-16	100.0
									PP	2.3E-11	99.7

SNV, single nucleotide variant; Chr, chromosome; SIFT, Sorting Intolerant from Tolerant algorithm which predicts the effect of coding variants on protein function; Polyphen, Polymorphism Phenotyping tool predicts possible impact of an amino acid substitution on the structure and function of a human protein; Posterior probability, the SNV's accounted posterior probability of driving the blood pressure association under the annotation-informed prior.

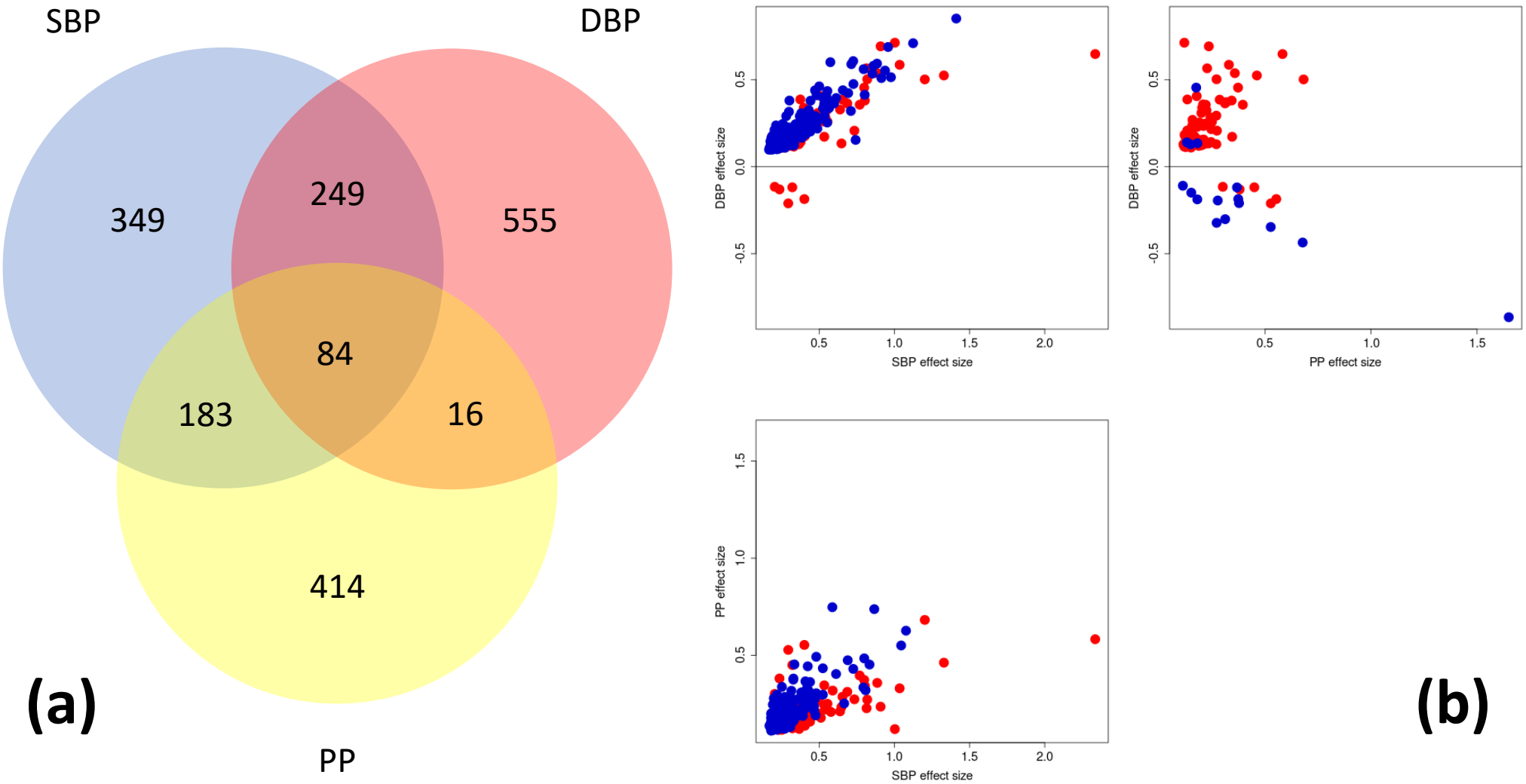

Figure 1. Overlap of 1,850 distinct signals attaining genome-wide significant evidence of association with SBP, DBP and PP in meta-analysis of BP GWAS in up to 757,601 individuals of European ancestry. (a) Venn diagram showing the number of signals shared across BP traits. Sharing of signals across traits is much more common between SBP and DBP or SBP and PP, with just 16 associations shared between only DBP and PP. (b) Comparison of allelic effect sizes on SBP, DBP and PP for the index SNV at the 532 distinct association signals that are shared across multiple BP traits. The effect has been aligned to the SBP or PP increasing allele for the signal. Blue points correspond to the 448 association signals that are shared across exactly two BP traits, whilst red points correspond to the 84 association signals that are shared across all three BP traits. When signals are shared between SBP and PP, the direction of effect of the index SNV on the traits is always concordant.

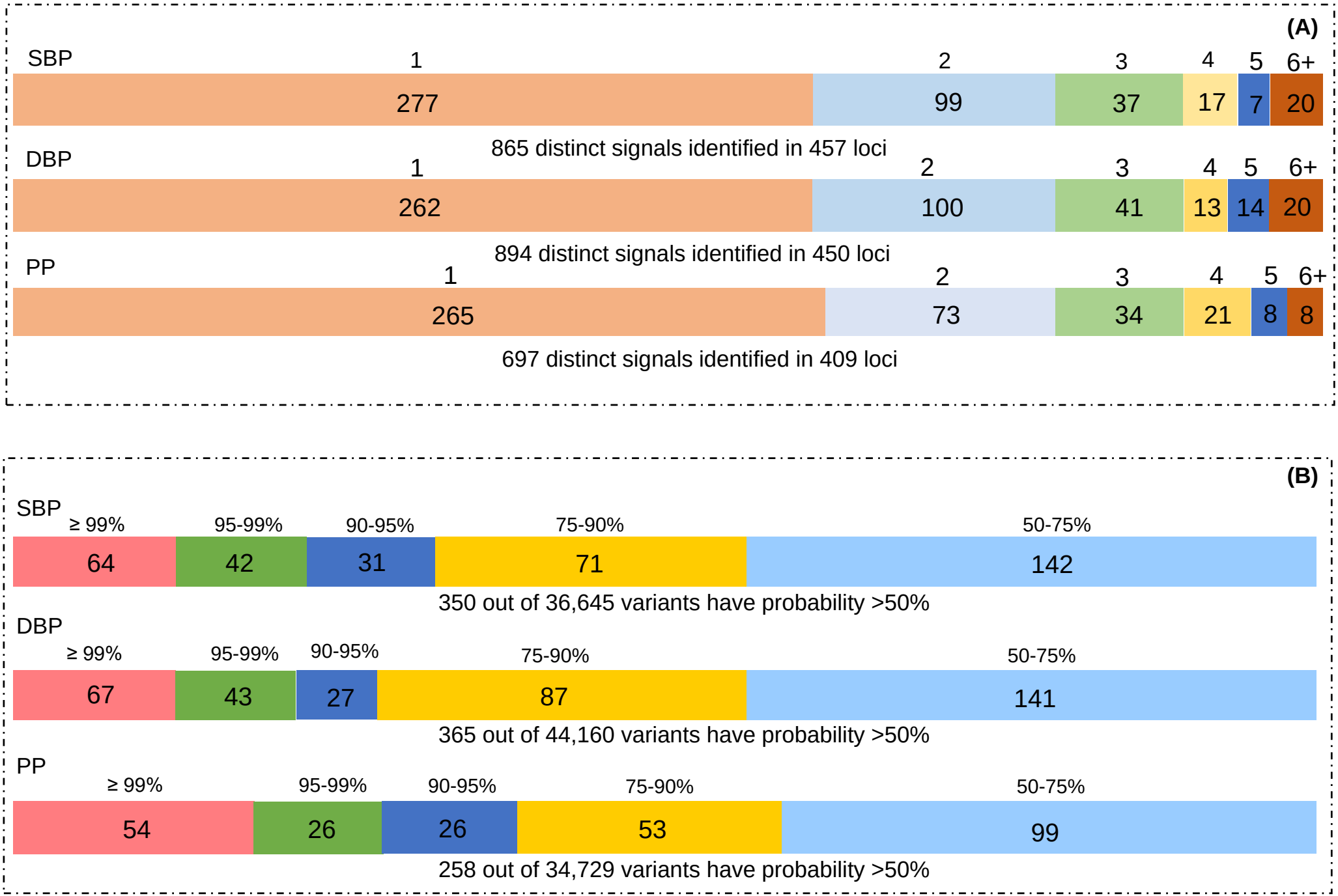
(A)
SBP
1
2
3
4
5
6+
277
99
37
17
7
20
865 distinct signals identified in 457 loci
DBP
1
2
3
4
5
6+
262
100
41
13
14
20
894 distinct signals identified in 450 loci
PP
1
2
3
4
5
6+
265
73
34
21
8
8
697 distinct signals identified in 409 loci
(B)
SBP
≥ 99%
95-99%
90-95%
75-90%
50-75%
64
42
31
71
142
350 out of 36,645 variants have probability >50%
DBP
≥ 99%
95-99%
90-95%
75-90%
50-75%
67
43
27
87
141
365 out of 44,160 variants have probability >50%
PP
≥ 99%
95-99%
90-95%
75-90%
50-75%
54
26
26
53
99
258 out of 34,729 variants have probability >50%

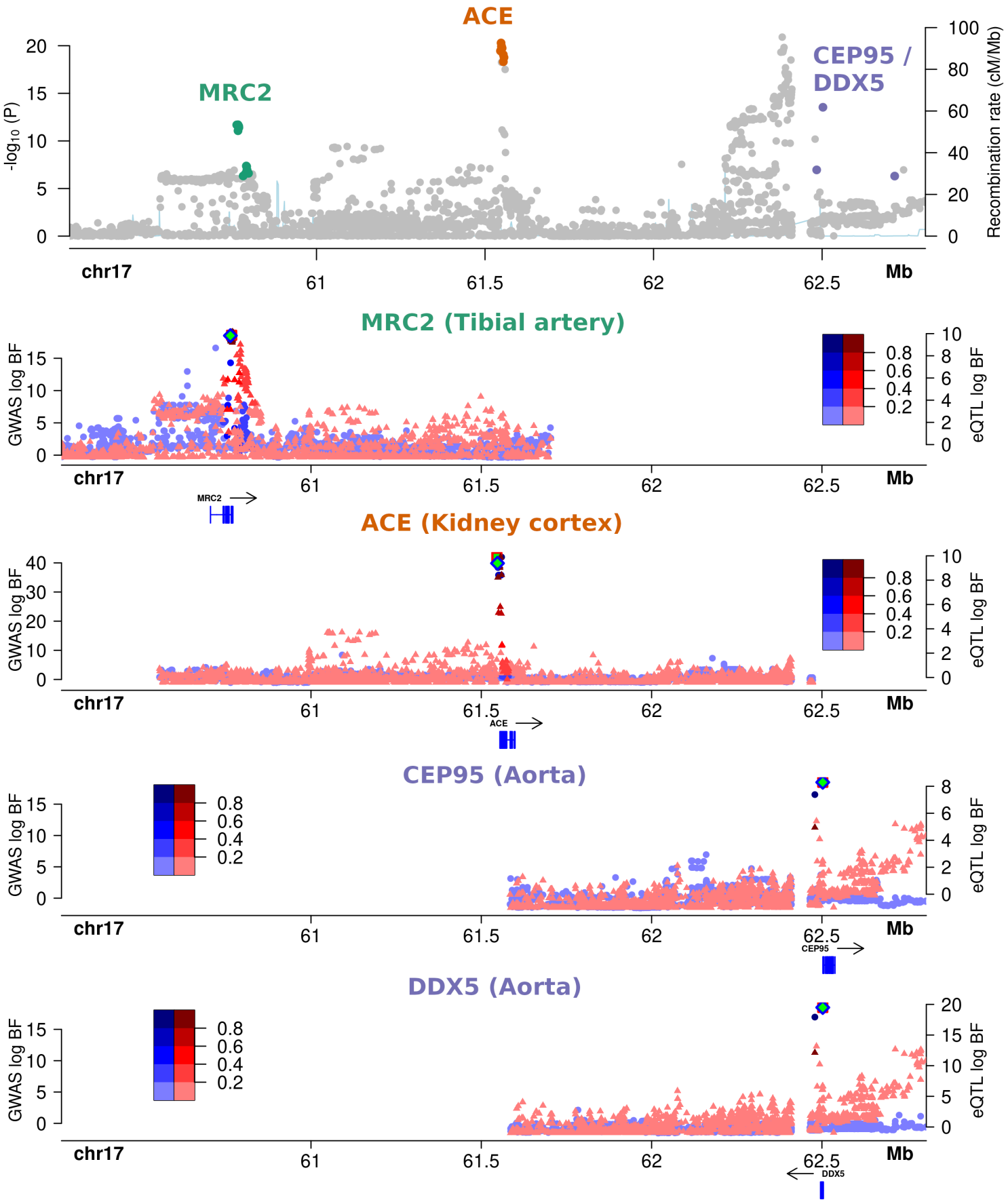

Meta-analysis of 757,601 individuals of European ancestry

SBP, DBP, PP

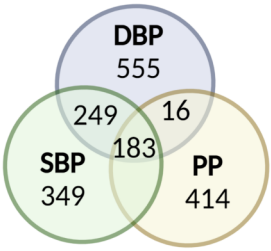

606 genomic regions → **1850 distinct signals**

Annotated fine-mapping and computational approaches

	SBP	DBP	PP
High-confidence missense variant	30 signals	37 signals	21 signals
Colocalised eQTL	96 signals	107 signals	84 signals
Promoter-capture Hi-C	281 signals	303 signals	231 signals
Candidate Effector Genes (at least one line of evidence)	**956**	**900**	**773**

Additional supportive evidence

Mouse model

Human cardiovascular and renal phenotypes

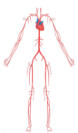

Gene and protein expression

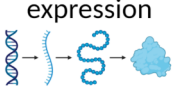

Consolidated Effector Genes (two or more additional lines of evidence)

SBP	DBP	PP
197	**184**	**180**

Enrichment analysis